Spatiotemporal distribution of aerosols over the Indian subcontinent and its dependence on prevailing meteorological conditions

Sinan Nizar[1] · B. M. Dodamani[1]

Abstract

The prevailing meteorological conditions that influence the advection and diffusion of the atmosphere govern the distribution of atmospheric particles from its sources. The present study explores the spatiotemporal distribution of atmospheric aerosols over the Indian subcontinent (5°–40° N, 65°–100° E) and its dependence on the prevailing meteorological conditions. Eleven years (2002–2012) of Aerosol Optical Depth (AOD) obtained from the Moderate Resolution Imaging Spectroradiometer (MODIS) along with meteorological parameters extracted from reanalysis data are analysed at monthly timescales. Wind speed, wind divergence and planetary boundary layer height (PBLH) are studied as parameters for advection and diffusion of atmospheric aerosols. The result shows higher aerosol loading during the monsoon season with increased spatial variability. Wind speed and divergence correlate with AOD values both over land ($R = 0.75$) and ocean ($R = 0.82$) with increased aerosol loading at higher wind speeds, which are converging in nature. Owing to the varied climatology of the Indian subcontinent, land and ocean areas were classified into subregions. Analysis was carried out over these subregions to infer the influence of meteorological conditions on aerosol loading. Results are indicative of a distinct characteristic in the prevailing meteorological conditions that influence the distribution of certain aerosol types. Further, the PBLH was analysed as an indicator of atmospheric diffusion to infer its importance in aerosol distribution. The results indicate that PBLH explains almost 30 to 90% of the total variance in AOD over the subregions which is particularly evident during the winter and pre-monsoon seasons.

Keywords Aerosol · Meteorology · Wind speed · Wind divergence · Planetary boundary layer height · India

Introduction

Aerosols are suspended solid or liquid particles in the Earth's atmosphere. Though short-lived, their presence is always felt in the atmosphere due to numerous anthropogenic and natural sources. Wind advects these particles from their sources rendering a heterogeneous distribution over the globe. The complex interaction of these atmospheric particles with solar radiation has acknowledged their importance in radiation budget and hence climate dynamics. Unlike the greenhouse gases, aerosols cause a reduction in solar radiation reaching the Earth's surface through a variety of complex radiative and microphysical processes (Schwartz 1996; Ramanathan et al. 1990; Guleria and Kuniyal 2013; Guleria and Kuniyal 2016). Depending on their size, they may absorb and/or scatter longwave and shortwave radiations (Chylek and Coakley 1974; Penner et al. 2001). As cloud condensation nuclei, they also influence cloud lifetime and cloud microphysics such as quantity, phase and size (Twomey 1977; Seinfeld and Pandis 2006; Li et al. 2017). These interactions suppress precipitation and tend to spin down the hydrologic cycle (Ramanathan et al. 1990). Besides these atmospheric interactions, aerosols are also associated with adverse impact on human health (Hoek et al. 2002; Pope et al. 2004; WHO 2013; Fuzzi et al. 2015) and agriculture (Ainsworth and Long 2004).

The Indian summer monsoon (June–September) which can be perceived as a gigantic convection system produced by differential seasonal heating of the continental and the surrounding oceanic areas contributes about 80% of the average annual rainfall in India. With a profound influence of aerosols

✉ Sinan Nizar
zinan.dx@gmail.com

B. M. Dodamani
bm.dodamani@gmail.com

[1] Department of Applied Mechanics and Hydraulics, National Institute of Technology Karnataka, Surathkal, Mangalore 575025, India

even on this large-scale circulation (Wang 2004; Ramanathan et al. 2005; Lau et al. 2008), it is important to understand the spatiotemporal distribution of atmospheric aerosols. Remote sensing of aerosols using satellite and ground-based sensors perceived the spatial and temporal distribution of aerosols over the globe. Being the second most populated country and a host of varied geographic features, India experiences differential aerosol loading from numerous natural and anthropogenic sources. In general, northern India (20°–30° N) is subjected to heavier aerosol loading when compared to southern India. The Indo-Gangetic Plains (IGP) in northern India is the major hotspot of aerosol loading (Washington et al. 2003; Dey 2004; Gautam et al. 2009a, b). Dust aerosols transported from the Thar Desert in western India and eastern Pakistan mixed with regional anthropogenic aerosols are the major contributors to IGP aerosol loading (Pease et al. 1998; Prospero 2002; Singh et al. 2004). Spatial gradients in aerosol loading are also observed with the difference in topography such as near the foothills of Himalayas (Gautam et al. 2009a, b). The Indian Ocean bordered by the densely populated Indian mainland is a good example of aerosol transportation from polluted continental areas to relatively cleaner ocean areas. The Arabian Sea in the west and the Bay of Bengal to the east show varied aerosol distribution depending on prevailing meteorology and proximity to sources (Rajeev et al. 2000; Kalapureddy et al. 2009; Kaskaoutis et al. 2009, 2010; Badarinath et al. 2010).

The spatial and temporal distribution of aerosols strongly depends on the distribution of sources/sinks and how these interact with transport. Aerosol transportation and its distribution are also governed by the prevailing meteorological conditions (Zhao et al. 2010). Meteorological parameters such as wind speed and direction, temperature, relative humidity and precipitation determine the extent of vertical redistribution and long-range transport of atmospheric particles. Thus, depending on these parameters, aerosols may accumulate or disperse in a region (Cheng et al. 2007). Many studies have been carried out to understand the influence of weather conditions on the distribution of particles in the atmosphere (Tanner and Law 2002; Ding et al. 2004; Zheng et al. 2015; Kaskaoutis et al. 2017). Moorthy and Satheesh (2000) explored the influence of wind speed on daily AOD at Minicoy in the Arabian Sea and found an exponentially increasing relationship. Though this remote island is influenced by continental aerosols during certain months, the exponential relation is mainly attributed to higher wind speeds contributing to marine aerosol production.

Using reanalysis wind data and MODIS aerosol product, Aloysius et al. (2008) showed that wind convergence over the Ganga basin is the major factor causing heavy aerosol concentration. Further, they used the flux-continuity equation to estimate the transported aerosols and then the aerosols source/ sink strength over the Ganga basin. Not only the advection of

aerosols by wind and its redistribution based on convergence but also the diffusion of these particles during their residence in the atmosphere is an important parameter. The meteorological conditions that are unfavourable for diffusion causing air pollution in an urban environment were presented by Ziomas et al. (1995). Wang et al. (2016) investigated the influence of atmospheric diffusion conditions on air quality in China. Daily PBLH, surface wind speed and precipitation were used as indicators for air stagnation, describing the atmospheric diffusion capability. Their results showed that favourable atmospheric diffusion conditions contributed to approximately 40% of the total decreased concentrations during winter.

The aforementioned literature (Ziomas et al. 1995; Moorthy and Satheesh 2000; Rajeev et al. 2000; Tanner and Law 2002; Ding et al. 2004; Cheng et al. 2007; Aloysius et al. 2008; Zhao et al. 2010; Zheng et al. 2015; Wang et al. 2016) suggests the importance of prevailing meteorological parameters in regulating the transport of atmospheric particles. This provides knowledge in improving the prediction of aerosol concentration over the globe. For a developing economy like India, anthropogenic aerosol sources are rising owing to urbanisation and industrialisation. This necessitates the understanding of spatial redistribution of aerosols from their sources. Various literature (Moorthy and Satheesh 2000; Aloysius et al. 2008; Chitranshi et al. 2015) have studied the influence of meteorological parameters such as wind speed, direction and divergence on aerosol distribution over the Indian subcontinent. But these parameters are indicative of atmospheric advection, whereas the diffusion of atmospheric particles is also an important factor (Ziomas et al. 1995; Quan et al. 2013; Wang et al. 2016). The present study tries to investigate the influence of meteorological parameters indicating both advection (wind speed and divergence) and diffusion (PBLH) on spatiotemporal distribution of aerosols over the Indian subcontinent and the adjacent Indian Ocean.

Meteorological parameters such as wind speed, divergence and PBLH from reanalysis data are studied for their possible influence on AOD obtained from MODIS data. The "Introduction" section provides an overview of the various literature. The "Data and methodology" section describes the data and methodology used in this study. In the "Results and discussion" section, the spatiotemporal climatology of aerosols and the meteorological parameters are discussed. The variation of AOD with meteorological parameters over different regions of the study area is also discussed in this section followed by the implications of the results and a summary of major conclusions in the "Conclusions" section.

Data and methodology

The data used and the methodology adopted for the study are described in this section. The study considers the region

between 5° N to 40° N and 65° E to 100° E bounding the Indian mainland and adjacent oceans for 11 years from 2002 to 2012.

Aerosol data

Though point measurements provide a refined view of aerosol characteristics on a local scale, they are not necessarily representative of regional concentration. In this regard, satellites were established to be a decent tool to understand the broad spatiotemporal properties of aerosols and their accompanying effects from global to local scales (Misra et al. 2015). Terra and Aqua satellites on-board the Moderate Resolution Imaging Spectroradiometer provide global observations of AOD (Levy et al. 2010; Hsu et al. 2013). These observations provide daily insight into the global distribution of aerosol columnar content. MODIS AOD products have been extensively validated by numerous researchers (Tripathi et al. 2005; Choudhry et al. 2012; Sayer et al. 2013; Misra et al. 2015). Monthly average AOD (550 nm) from Collection 6.1, level 3 AOD products (1° × 1°) derived from Terra's MODIS measurements, is used in this study (Platnick et al. 2017). To ascertain the contribution of different aerosol types, the reanalysis dataset from the Modern-Era Retrospective analysis for Research and Applications, version 2 (MERRA 2; Gelaro et al. 2017) have been used. The AOD at 550 nm from dust (DU), sea salt (SS), black carbon (BC), organic carbon (OC) and sulphate (SU) aerosols are derived from the monthly mean aerosol diagnostics dataset (GMOA 2015b).

Meteorological data

The corresponding meteorological analyses implemented in this paper are based on the results of meteorological reanalysis products provided by the National Centre for Environmental Prediction (NCEP, Reanalysis 2), https://www.esrl.noaa.gov/psd/data/gridded/data.ncep.reanalysis2.pressure.html). For a complete understanding, we consider both the upper-air and surface circulation patterns. Wind field at various vertical levels was extracted from the NCEP Reanalysis data set on a 2.5° × 2.5° latitude/longitude grid on a monthly basis. As the PBLH has strong diurnal variation, its value during the time of passage of Terra over the Indian subcontinent was extracted at a spatial resolution of 1° × 1° from the MERRA 2 dataset (GMOA 2015a). Since the wind fields were available at 2.5° resolution, the present study was done at 2.5° × 2.5° with all data resampled to this resolution.

Methodology

The present study first focusses on the spatiotemporal distribution of 550 nm AOD and then analyses various meteorological parameters to investigate their possible influence. As

evident from the literature, the atmospheric transportation and the distribution of aerosols are governed by advection and diffusion. Thus, wind speed and divergence are used as indicators for advection, whereas the PBLH is used as an indicator of atmospheric stability and hence atmospheric diffusion. Eleven years (2002–2012) of aerosol climatology during the winter (January–February), pre-monsoon (March–May), monsoon (June–September) and post-monsoon (October–December) season is presented in this paper. Spatial plots of mean seasonal AOD was derived from monthly AOD over the Indian subcontinent bounded between 40° and 5° north latitudes and 65° and 100° east latitudes. The mean seasonal AOD for each grid was derived from the AOD for a month m in the year $y(AOD_{m,\,y})$ in a given season for that particular grid as:

$$AOD_{\text{season}} = \frac{\sum\limits_{m=1}^{n} AOD_{m,y}}{n} \tag{1}$$

where n is the total number of months of MODIS data during a given season over all the 11 years of data. Pixels with missing data values during the period were left as no data pixels. As the land areas inhibited higher aerosol loading in comparison to the oceanic areas, all the proceeding analyses were carried out separately over the land and ocean. Temporal variation of AOD was plotted from the spatially averaged AOD $\left(\overline{AOD}_{\text{month}}\right)$ for each month over the land and ocean separately as:

$$\left(\overline{AOD}_{\text{month}}\right) = \frac{\sum AOD}{n} \tag{2}$$

where AOD is the AOD value at each pixel with data value and n is the total number of pixels with data value over the land or ocean in that particular month. Each pixel was classified as land if 50% or more area of the pixel corresponded to land or else as the ocean. Temporal variations of $\overline{AOD}_{\text{month}}$ for over 132 months starting from January 2002 are presented in this study. To study the monthly spatial variation of AOD, standard deviations were also plotted along with each monthly values. This represents the spatial variations of AOD during each month.

Meteorological parameters derived from reanalysis data were then analysed. Monthly values of zonal (u) and meridional (v) wind components were extracted at different vertical levels and the resultant wind speeds were calculated for every 2.5° × 2.5° pixel. To account for the inflow and outflow of air masses, the wind divergence was also studied. The wind divergence was computed from the horizontal wind components as described by McNoldy (2004) using the formula

$$\text{Divergence} = \frac{\partial u}{r\cos\varphi\,\partial\lambda} + \frac{\partial(v\cos\varphi)}{r\cos\varphi\,\partial\varphi} \tag{3}$$

where φ and λ are latitude and longitude and r is the Earth's radius. Similar to the wind speed, the wind divergence was also computed at different vertical levels at the same spatial resolution. As the horizontal length scale of each grid (≈ 277 km) is much larger than the vertical perturbations over the land (≈ 10 km), this equation is applied both over the land and ocean. Temporal variation of these meteorological parameters and their correlation with AOD was then investigated.

The Indian subcontinent being a host of varied climatology is further divided into subregions for further analysis. The whole Indian region is thus subdivided into seven subregions. The division is in accordance with Ramachandran and Cherian (2008) where he classified the region according to its geographic location. The locations and their bounds are shown in Fig. 1. Correlation analysis was then carried out over each subregion between AOD and each of the meteorological parameters. For the correlation analysis, only those grids where collocated values were available for each parameter were considered. These values of wind speed, divergence and PBLH were then sorted as a function of AOD and averaged to create a total of 50 scatter points. These values were then used for multiple regression analysis to ascertain their contribution to aerosol loading.

As the Indian subcontinent hosts a variety of aerosol types, AOD values for sea salt aerosol (SS), dust aerosol (DU), organic carbon aerosol (OC), black carbon aerosol (BC) and sulphate aerosol (SU) were derived from the MERRA-2 dataset to analyse the contribution of different aerosol types

to the total AOD. The total AOD (AOD_{Total}) values could roughly be fitted using the equation

$$AOD_{Total} = DU + BC + OC + SS + SU \tag{4}$$

Thus, the contribution of each aerosol type (AOD_s) can be calculated as

$$AOD_{contribution} = \frac{AOD_s}{AOD_{Total}} \tag{5}$$

The contribution of each aerosol type in difference meteorological conditions is analysed. In addition to this, proportional reduction in error (PRE; Judd et al. 2009) was also calculated from the residuals of regression analysis.

$$PRE = \frac{\sum E(B)^2 - \sum E(A)^2}{\sum E(B)^2} \tag{6}$$

where $E(B)$ is the residual in a model excluding PBLH and $E(A)$ is the residual in a model involving all the three parameters. The PRE helps to identify the contribution of PBLH in defining the variations in AOD.

Multiple trajectories at different locations over the land and ocean were computed using the PC-Windows-based NOAA HYSPLIT model (Stein et al. 2015; Rolph et al. 2017). The locations over the land and ocean were selected based on the aerosol loading and 4-day multiple backward trajectories were computed at different vertical levels. As the Terra overpasses the study region around 12:00, trajectories were calculated

Fig. 1 Location of different subregions in the study area
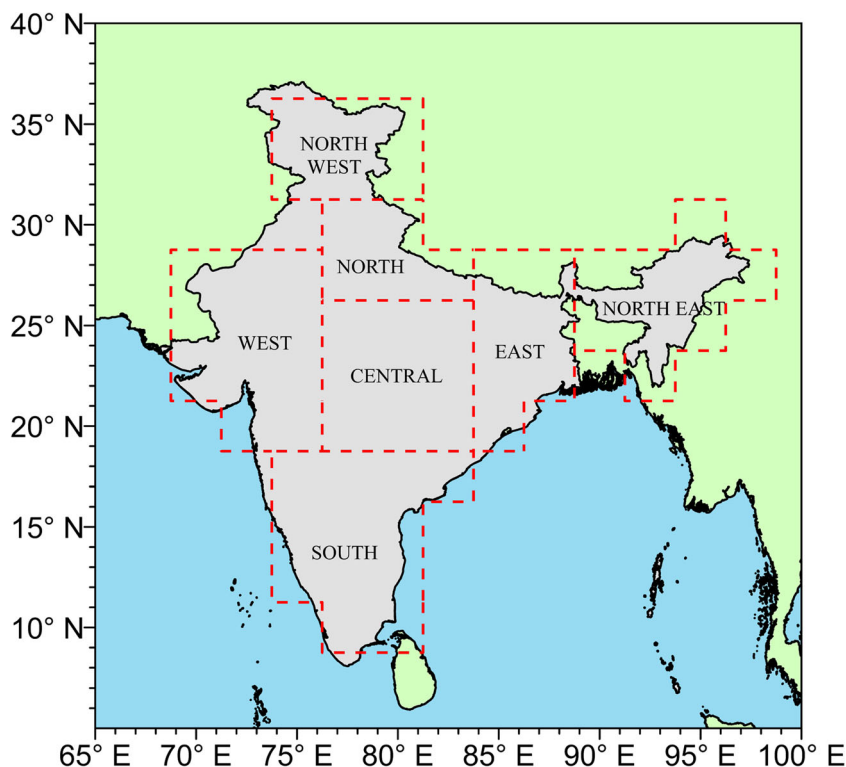
starting at every 12:00 for a year. The daily NCEP reanalysis data with a resolution of $2.5° \times 2.5°$ was used for this analysis. Trajectory frequency was then computed from these 365 backward trajectories to investigate further how frequently the air masses are drawn from a region. The frequencies are computed over an arbitrary grid over the computational domain by counting the number of trajectory intersections over each grid cell and normalising by the number of trajectories. Further, trajectory clusters for the highest loaded month for these locations were also computed. Both the locations experienced highest AOD loading during May 2011 and trajectories during this month were clustered to show potential aerosol transport pathways.

Results and discussion

Spatial distribution of AOD

Before investigating the link between aerosol concentration and prevailing meteorological conditions, it is necessary to study its spatiotemporal distribution over the region. The spatial distribution of AOD highlighting the spatial variability over the Indian subcontinent is presented in Fig. 2. As mentioned in the literature (Washington et al. 2003; Dey 2004), the dominance of aerosols over northern India especially the IGP is visible. Heavy aerosol loading over the Thar Desert in western India and eastern Pakistan is transported over northern India along the IGP and is eventually spread over the Bay of Bengal in the eastern Indian Ocean. Thus, a vivid picture of aerosol transportation from the arid regions is depicted. Similar to the observations by Gautam et al. (2009a, b), a significant reduction in aerosol concentration in contrast to IGP is observed over the foothills of the Himalayas and the Tibetan Plateau. Such spatial gradients with topographical differences are also visible over the Aravali, Eastern Ghats and the Western Ghats mountain ranges. Apart from the IGP, certain regions of central India (19° N, 76° E) show high aerosol loading when compared to the surrounding areas. It is interesting to note that these regions are bounded by the Western Ghats to the west and south, Satpura ranges to the north and the Eastern Ghats to the east. Hindrance to flow caused by the surrounding mountain ranges transporting aerosols to higher altitudes near its foothills could be a factor for increasing the aerosol loading.

The influence of continental aerosols on the adjacent oceanic regions can be inferred as most of the heavier aerosol concentrations are observed along the coast and weaken as the distance from the land increases. Over the Bay of Bengal, aerosol loading along the east coast can be seen as an extension of the IGP aerosol loading. Thus, most of the aerosols are dust mixed with anthropogenic aerosols from IGP (Guttikunda et al. 2003; Monkkonen 2004). Though not as heavy as the east coast, the west coast shows wider aerosol loading over the Arabian Sea. Apart from the continental sources, the oceanic regions are also influenced by marine traffic (Nair et al. 2008). The Indian coastline spanning over 7500 km houses 12 major and 200 minor ports. These ports handle about 95% of India's trading by volume and 68% by value (Ministry of Shipping 2016). Ship-borne measurements from the Integrated Campaign for Aerosol, Gases and Radiation Budget (ICARB) reported a significant increase in aerosol abundance from heavy shipping in the oceanic region (Nair et al. 2008). Anthropogenic aerosol loading over the adjoining ocean region in the west coast of India was also shown by Srivastava et al. (2016). Thus, marine traffic along with continental aerosols is responsible for aerosol loading over the oceanic regions. Though a general picture of the seasonal climatological mean of AOD is depicted in Fig. 2, there also exists annual variations in spatial distributions. The dependence of such distributions on the climatological conditions is discussed in "Meteorological characteristics over regions of high and low AOD" Section.

Owing to increased aerosol sources of natural and anthropogenic origin, land areas are heavily loaded in comparison to the surrounding ocean. Not only the distribution of sources but also the variety topography influences the aerosol distribution over land, whereas such influences are absent over the ocean. The results indicate that average AOD values over land (0.40) are almost 30% more than those over the ocean (0.30) for the 11 years under consideration.

Temporal distribution of AOD

Apart from the spatial variability, there also exists a temporal variation in AOD. The spatial averages over land and oceanic regions were calculated for each month. This enables to study the temporal changes in average aerosol concentrations. The monthly variation in the average daily AOD over land and ocean along with the standard deviation is given in Fig. 3. Both land and ocean show a strong seasonal variation of AOD with increased aerosol loading during the monsoon months of June, July and August. Standard deviations about the monthly spatial means are also plotted to show its spatial variation. It can be observed that there is not only an increase in average AOD but also an increase in the spatial variability among the pixels during the monsoon season. This suggests that the increased aerosol loading during the monsoon season is concentrated in particular locations. The AOD over the oceanic areas is substantially lower than those over land areas. Moreover, the oceanic areas also experience less spatial variability as shown by the standard deviation bars.
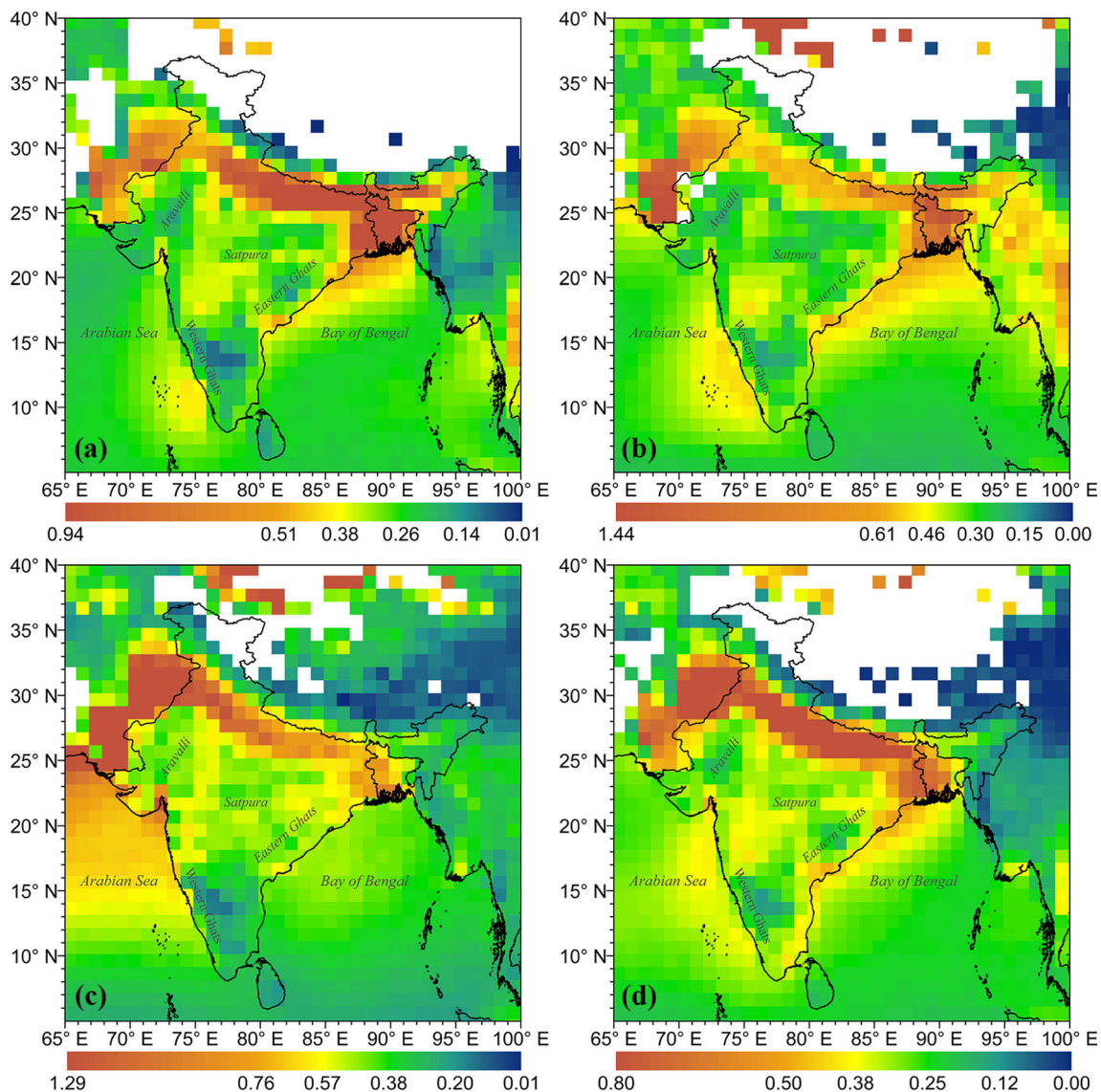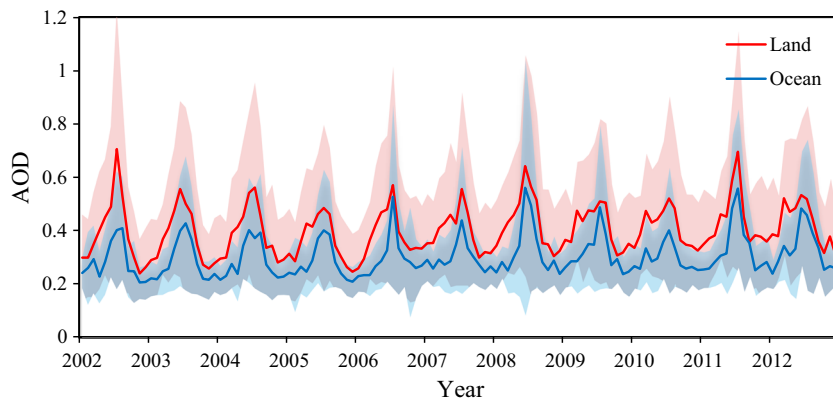
Fig. 2 Spatial distribution of seasonal AOD from MODIS averaged during 2002–2012. **a** Winter. **b** Pre-monsoon. **c** Monsoon. **d** Post-monsoon

Fig. 3 Monthly variation of average daily AOD over the land and ocean from 2002 to 2012

Meteorological characteristics

Given the spatiotemporal distribution of AOD, knowledge about the variations in meteorological characteristics is required to link their relationship. Thus, the monthly variation in the meteorological parameters such as wind speed and divergence are presented in this section.

Wind speed

Due to the vertical gradient of horizontal wind speed in the atmosphere, the wind speeds at different vertical levels have been studied. The temporal distribution of the average wind speed at different vertical levels over land is shown in Fig. 4a. Though the wind speed increases with altitude, there is a similar seasonal pattern up to 850 hPa with higher wind speeds during the monsoon season similar to the AOD distribution. It is also observed that during the monsoon season, the difference in wind speeds at the different levels increases compared to that in other months similar to the variation in the standard deviation of AOD. Thus, the monsoon season witnesses stronger wind speeds with distinct vertical gradients. The wind speed over the ocean is relatively higher compared to that over land but shows a similar seasonal variation (Fig. 4b). This is due to the lesser surface roughness over the oceanic areas.
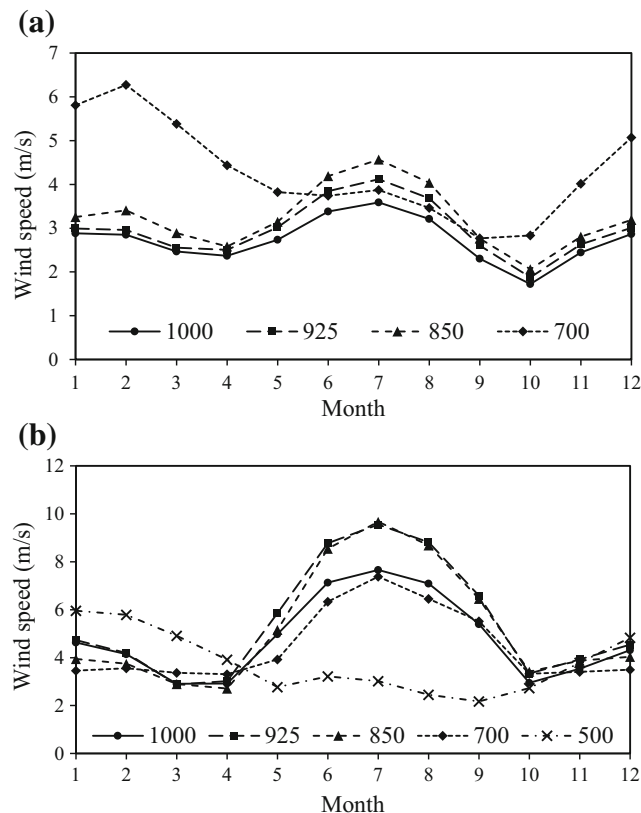
Unlike land, the ocean shows similar patterns in wind speed even up to 700 hPa.

Divergence

Wind divergence is indicative of the accumulation or dispersion of atmospheric particles in a region. Temporal distribution of wind divergence at different vertical levels is shown in Fig. 5. Over the land (Fig. 5a), divergence during the winter season decreases towards the summer and eventually becomes convergence (negative divergence) during the monsoon season. Similar to wind speed, the divergence over the land up to a height of 850 hPa shows similar patterns. Unlike land, the ocean experiences increasing divergence during the monsoon season (Fig. 5b). Overall, the wind speed and divergence over the land and ocean are characterised with seasonal variations with the monsoon season witnessing higher wind speeds with converging air masses over the land and diverging air masses over the ocean.

Variation of AOD with meteorological parameters

Having said that both AOD and meteorological parameters such as wind speed and divergence exhibit seasonal variation, their correlation was investigated. Figure 6a shows the monthly variation in AOD along with wind speed over the land.
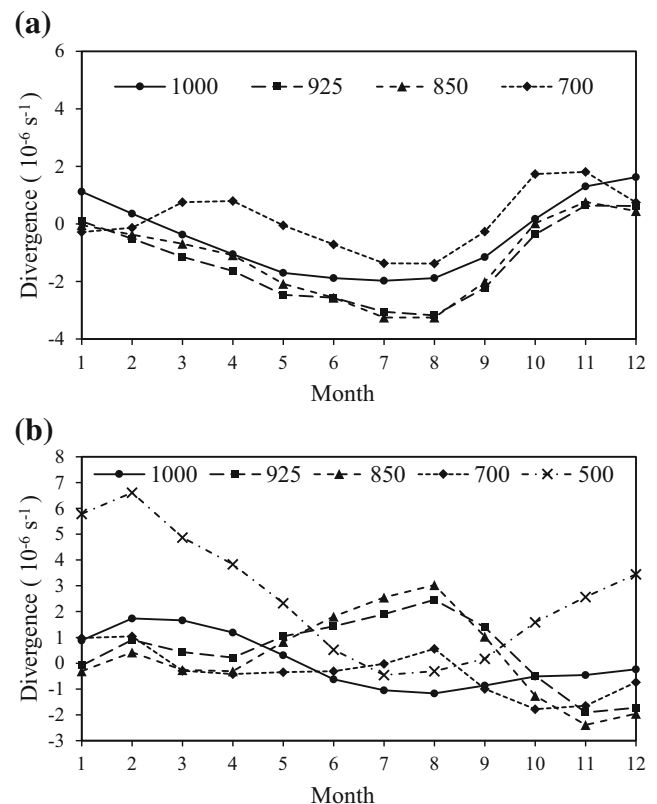

Fig. 4 Monthly variation of average wind speed at different pressure levels (hPa) over the land (**a**) and ocean (**b**) from 2002 to 2012

Fig. 5 Monthly variation of wind divergence at different pressure levels (hPa) over the land (**a**) and ocean (**b**) from 2002 to 2012

(a)

a

(b)

b

Fig. 6 Temporal variation of average daily AOD with **a** wind speed and **b** divergence at 850 hPa over the land from 2002 to 2012
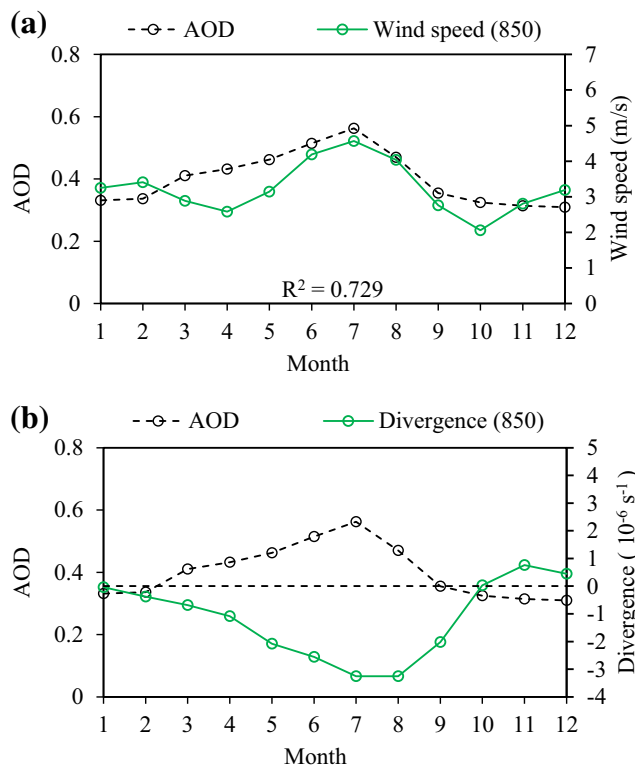
Fig. 7 Temporal variation of average daily AOD with **a** wind speed and **b** divergence at 850 hPa over the ocean from 2002 to 2012

Wind speed and AODs show similar temporal variation with higher values during the monsoon season. Thus, AOD values over land increase with an increase in wind speed. The variation of AOD along with wind divergence is shown in Fig. 6b. The monsoon season with higher AOD values is characterised by negative wind divergence. A multiple regression analysis of wind speed and divergence with AOD using the 11 years of monthly data (132 data points) shows a good correlation as indicated by the correlation coefficient (R). The correlation varies at different vertical levels with a maximum of 0.75 at 850 hPa.

Over the ocean, a more vivid relationship is observable. AOD and wind speed (850 hPa) exhibit a higher correlation ($R = 0.82$), whereas a clear divergence can be seen during the monsoon season (Fig. 7). This increased correlation is due to the relatively pristine ocean areas which are loaded mostly by transported continental aerosols in comparison to the numerous aerosol sources over the land.

Both land and ocean show an increasing correlation of wind speed and AOD at higher vertical levels with a maximum occurring at 850 hPa. This expresses the importance of wind direction and air mass trajectories with different areal influence. This was further investigated by running multiple backward trajectories at different vertical levels. Previous studies have also used trajectory analysis to infer the sources and locations of aerosols (Nair et al. 2008; Giles et al. 2011; Kedia et al. 2014). The frequency of backward trajectories at
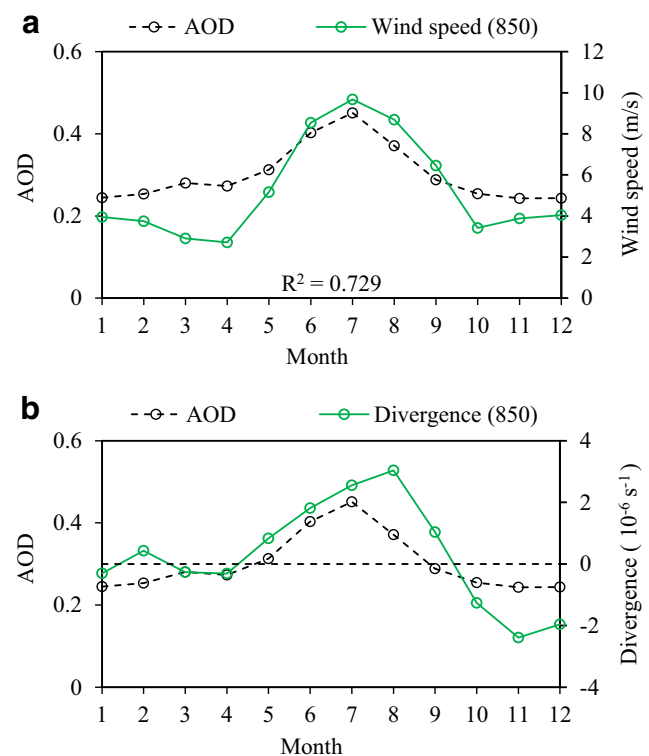
near surface (1000 hPa) and mid-tropospheric (850 hPa) levels over the land and ocean was plotted (Fig. 8a–d). The locations for computing trajectories were decided from among regions of heavy aerosol loading. Thus, over the land, a location at IGP (26° N, 83° E) and, over the ocean, a location near east coast (20° N, 88° E) were selected as shown in Fig. 8. Though both near surface (Fig. 8a) and mid-tropospheric (Fig. 8b) trajectories show similar frequencies over IGP, the 850 hPa trajectories are more frequently driven from the arid regions such as the Thar Desert. Thus, the 850 hPa trajectories not only accounts for surface aerosol movement but also for the elevated mid-tropospheric aerosols from farther areas. Over the ocean, there is more frequency of winds blowing from the adjacent land areas at 850 hPa when compared to 1000 hPa (Fig. 8c–d). To further validate the importance of mid-tropospheric wind, multiple backward trajectories at these locations were carried out for the month with the highest aerosol loading. Both the locations experienced highest AOD during May of 2011. Daily backward trajectories during this month were clustered and the results are presented in Fig. 9. It is evident that the trajectories at 850 hPa are driven from the arid regions bringing in dust aerosols and resulting in heavier aerosol loading. Over the ocean, the backward trajectories at 1000 hPa are confined over the ocean, whereas the 850 hPa are driven over the land surface. Thus, an increase in correlation with altitude can be inferred as the trajectories extending to land masses contributing to most of the oceanic aerosols.

Fig. 8 Trajectory frequency for 2013 over the land and ocean at different vertical levels

| > 100% | > 10% | > 1.0% | > 0.1% |
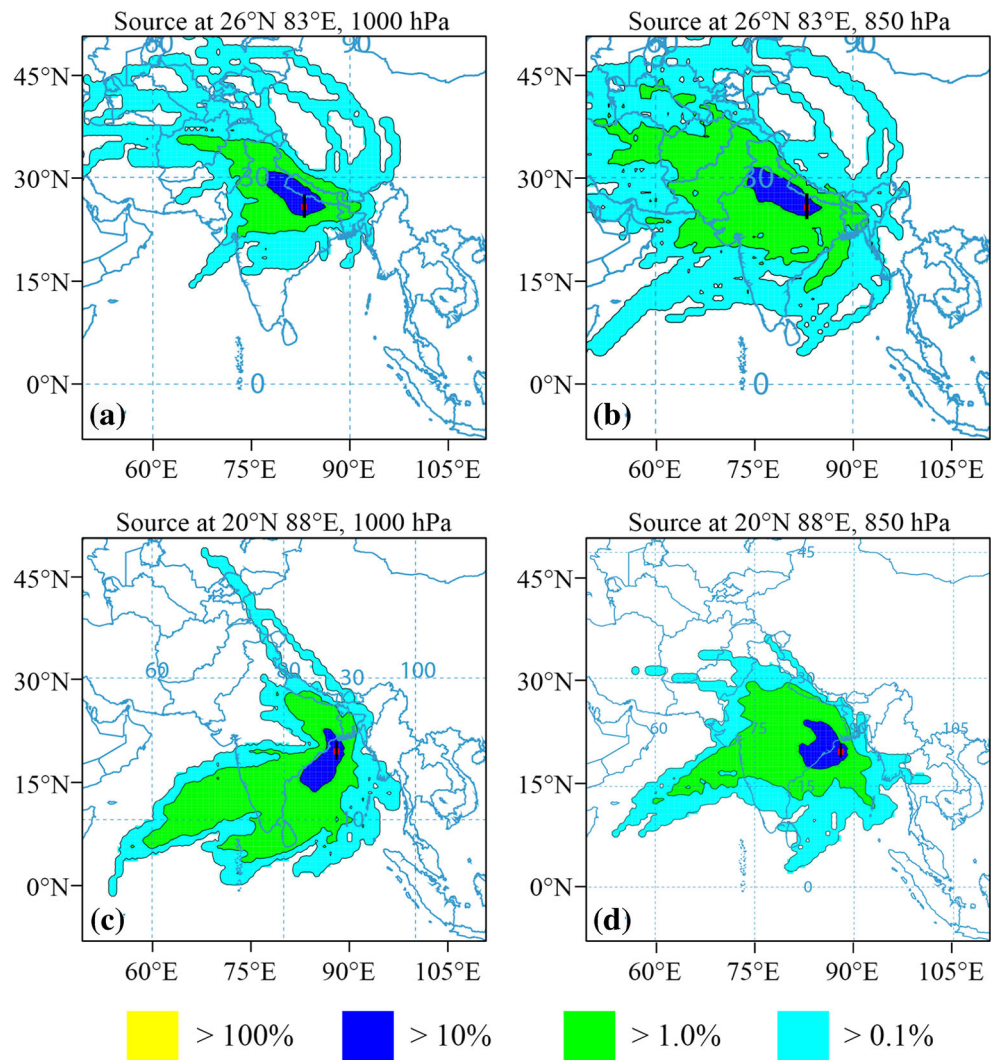
Meteorological characteristics over regions of high and low AOD

Apart from the seasonality in overall aerosol loading, there is also evidence of large spatial variability as seen in previous sections. This suggests that the increased aerosol loading over the Indian subcontinent is concentrated to particular locations within the region. Thus, aerosol concentrations were analysed to understand its dependence on meteorological conditions. For this purpose, the land and oceanic regions were classified into subregions, and the variation of meteorological parameters with AOD was analysed. As the literature suggests the importance of atmospheric diffusion in aerosol redistribution, PBLH has also been studied as an indicator of atmospheric stability. Thus, wind speed, divergence and PBLH were analysed as an indicative parameter for atmospheric advection and diffusion.

The figures showing the seasonal variation of wind speed, divergence and PBLH with AOD over the subregions are provided as supplementary files. The trends of each parameter along with the P value is summarised in Tables 1, 2, and 3. The northwest subregion has been omitted due to a large amount of missing data. The parameters exhibit distinct patterns not only over different subregions but also over the same subregion during different seasons. For example, the wind speed over the south subregion shows a decreasing trend with increasing AOD during the winter, whereas the monsoon witnesses increasing wind speed with AOD. Thus, winter season over the south subregion is characterised by heavier aerosol loading over regions of lower wind speed, whereas regions with high wind speed experience heavier aerosol loading during monsoon. This is because the Indian subcontinent hosts different aerosol types with each aerosol type having different climatology.

The AOD over the subregions experience varying contributions from each aerosol type during the seasons. The contribution of each aerosol type towards the total AOD over the subregions during different seasons is shown in Table 4. The south subregion during the winter season is characterised by significantly decreasing PBLH, significantly increasing
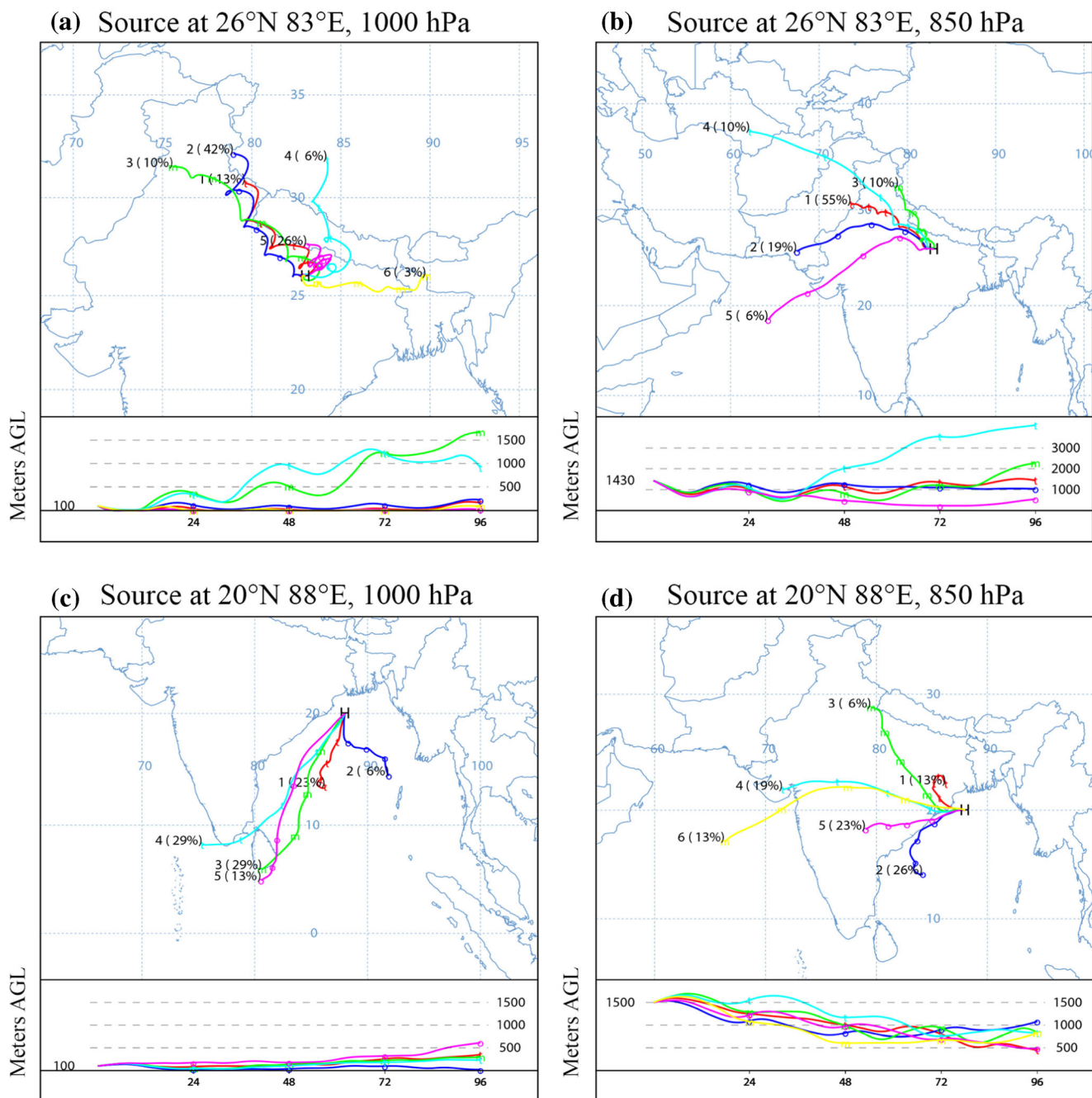
(a) Source at 26°N 83°E, 1000 hPa

(b) Source at 26°N 83°E, 850 hPa

(c) Source at 20°N 88°E, 1000 hPa

(d) Source at 20°N 88°E, 850 hPa

Fig. 9 Trajectory cluster for May 2011 over the land and ocean at different vertical levels

divergence and significantly decreasing wind speed with increasing aerosol loading. Thus, the south subregion during the winter experiences heavier aerosol loading in locations with lower PBLH and low wind speed which is diverging. However, it should be noted that the winter season has larger contribution from SU, BC and OC aerosols (84%) and less contribution from DU and SS aerosols (16%). AOD variation during the pre-monsoon is characterised by decreasing PBLH but is not significant as in winter. The wind divergence is increasing and is coupled with an increasing wind speed. The contribution of DU and SS aerosols (38%) during this

season is increased drastically along with a decrease in SU, BC and OC aerosols (62%). The variation of PBLH completely reverses with a significantly increasing trend with AOD during the monsoon season. Though the wind divergence during the monsoon is increasing as in the previous seasons, the wind speeds are significantly increasing with AOD. The contribution of DU and SS aerosols during this season is increased to 47% of the total AOD. Thus, there exists a pattern wherein lower PBLH and low wind speeds aid SU, BC and OC aerosols and higher PBLH and increased wind speeds aids DU and SS aerosols. This pattern can also be seen during the

Table 1 Trends in wind speed over the subregions during each season

Region	Winter		Pre-monsoon		Monsoon		Post-monsoon	
	Trend	P value	Trend	P value	Trend	P value	Trend	P value
S	−3.25	0.01	0.78	0.17	4.81	0.01	−3.44	0.01
W	0.25	0.82	6.33	0.01	3.38	0.01	0.46	0.41
N	0.27	0.63	3.26	0.01	0.86	0.03	1.44	0.01
C	−1.83	0.12	−1.28	0.22	2.93	0.01	−0.30	0.68
E	0.04	0.95	−1.54	0.01	−0.80	0.10	2.11	0.01
NE	−0.14	0.79	−2.17	0.01	0.78	0.20	−1.37	0.06
AS	−0.57	0.43	−0.77	0.08	3.14	0.05	−3.78	0.01
BoB	0.34	0.76	0.95	0.20	2.75	0.06	−1.14	0.28

post-monsoon season. Though not significant, the PBLH and wind speeds experience decreasing trends with AOD and are characterised by lower contribution by DU and SS aerosols (12%) and larger contribution from SU, BC and OC aerosols (88%).

The west subregion during the winter season is characterised by increasing PBLH, insignificant but increasing divergence and significantly increasing wind speed with increasing aerosol loading. This is similar to the conditions over the south during the monsoon season and exhibits similar contributions of aerosol types. With increasing PBLH and higher wind speeds, the DU and SS aerosols contribute about 35% of the total AOD. The increase in PBLH and wind speed becomes significant during the pre-monsoon season and results in an increased contribution from DU and SS aerosols (72%). Though the wind speed continues to be significantly increasing, the PBLH and wind divergence show a decreasing trend during the monsoon season. As a result, the contribution of DU and SS aerosols (63%) can be seen to deteriorate. As the post-monsoon season approaches, the wind speeds become insignificant with significantly decreasing PBLH. As a result, the season witnesses decreased contribution from DU and SS aerosols (24%) when compared to the previous seasons. The results contribute more validity to the dependence of aerosol types on meteorological condition wherein lower

PBLH and low wind speed aid SU, BC and OC aerosols and higher PBLH and increased wind speed aid DU and SS aerosols.

Similar patterns can also be observed over the north subregion. The winter season is characterised by decreasing PBLH, significantly increasing convergence and insignificantly varying wind speed with increasing aerosol loading. With decreasing PBLH and converging wind, the DU and SS aerosol contributions are low (23%) compared to other seasons. The PBLH and wind speed during the pre-monsoon season becomes significantly increasing with AOD, and as expected, the contributions of DU and SS aerosols are drastically increased (59%). The PBLH continues to be significantly increasing during the monsoon season but the wind speed though increasing becomes insignificant. This is reflected as a decrease in DU and SS aerosol contribution (46%). As the post-monsoon approaches, the PBLH becomes decreasing with decreased contribution from DU and SS aerosols (18%). Similar patterns can be observed over the central, east and north-east regions. Thus, in general, over the land, higher PBLH and higher wind speed support DU and SS aerosols, whereas lower PBLH and low wind speed support SU, BC and OC aerosols. This may be because increased wind speed and higher PBLH results in increased surface wind stress and

Table 2 Trends in wind divergence over the subregions during each season

Region	Winter		Pre-monsoon		Monsoon		Post-monsoon	
	Trend	P value	Trend	P value	Trend	P value	Trend	P value
S	8.80	0.01	4.41	0.01	2.24	0.23	0.83	0.72
W	7.97	0.21	7.02	0.10	−6.51	0.01	3.97	0.12
N	−14.3	0.01	−6.00	0.08	−4.65	0.01	−8.34	0.01
C	−23.9	0.01	−3.26	0.33	−4.68	0.09	−22.10	0.01
E	−8.83	0.01	0.15	0.95	−13.40	0.01	−6.37	0.01
NE	−4.13	0.45	−4.98	0.01	−1.81	0.31	−27.02	0.01
AS	21.15	0.01	8.50	0.01	−24.31	0.01	3.32	0.27
BoB	22.23	0.01	0.34	0.81	−20.63	0.01	33.76	0.01

Table 3 Trends in PBLH over the subregions during each season

Region	Winter		Pre-monsoon		Monsoon		Post-monsoon	
	Trend	P value	Trend	P value	Trend	P value	Trend	P value
S	−1747	0.01	−536	0.25	145	0.53	−273	0.24
W	1077	0.07	1379	0.01	−587	0.01	−1250	0.01
N	−599	0.03	2031	0.01	1179	0.01	−123	0.40
C	−364	0.53	864	0.01	−545	0.07	494	0.28
E	−1250	0.01	−1607	0.01	419	0.03	−392	0.01
NE	−535	0.03	564	0.01	81	0.55	−794	0.01
AS	−791	0.01	−714	0.01	−58	0.07	−356	0.01
BoB	−641	0.01	−639	0.01	−365	0.01	360	0.01

an unstable atmosphere with increased turbulence in turn supporting DU and SS aerosol production.

The oceanic regions show a different character. Both the AS and BoB are characterised by significantly decreasing PBLH with increasing AOD during the winter and pre-monsoon seasons. Thus, the increased aerosols concentrate over relatively stable atmospheric regions over the ocean. The contribution of SS aerosols (approx. 20%) remains low, whereas the continental aerosols have a higher contribution to the total AOD. These continental aerosols are mostly transported from the adjacent land areas and concentrate over stable oceanic regions with lower PBLH. As the monsoon season approaches, the wind speeds start to increase causing an increase in SS contribution both over the AS and BoB (39% and 41%).

Both the land and oceanic regions depict the importance of prevailing meteorological conditions in aerosol distribution. It is evident that not only the advection but also the diffusion of atmospheric particles is an important factor in aerosol distribution as indicated by the influence of PBLH. Further, the influence of atmospheric diffusion is quantified by evaluating the PRE of a multiple linear regression model. The results are tabulated in Table 5. The inclusion of PBLH in addition to wind speed and divergence shows significant PRE in most of

the cases. This is visible during the winter and pre-monsoon seasons. Higher temperature during the pre-monsoon season results in an unstable atmosphere with more influence on AOD. The PBLH during this season explains almost 30 to 90% of the variance in AOD over various regions. However, the PRE during the monsoon and post-monsoon seasons are lower and are due to the substantial reduction in the spatial variation of PBLH during these seasons. Thus, the atmospheric diffusion influences aerosol distribution especially during the winter and pre-monsoon seasons.

Conclusions

In the present study, spatiotemporal distribution of AOD over the Indian subcontinent and the surrounding Indian Ocean (5° N to 40° N and 65° E to 100° E) was studied to understand the possible influence of prevailing meteorological conditions. Eleven years (2002–2012) of MODIS AOD data along with wind speed, wind divergence and PBLH were investigated as parameters for advection and diffusion of atmospheric particles. These parameters derived from reanalysis data sets along with satellite-measured AOD values reveal distinctive characteristics over the land and ocean. Further, the study pertains to

Table 4 Contribution of various aerosol types to the total AOD inferred from MERRA 2 data

Region	Winter					Pre-monsoon					Monsoon					Post-monsoon				
	BC	DU	OC	SS	SU	BC	DU	OC	SS	SU	BC	DU	OC	SS	SU	BC	DU	OC	SS	SU
S	6	9	23	7	55	4	27	18	11	41	3	31	10	16	41	5	6	23	6	59
W	6	33	18	2	40	2	65	7	7	19	2	45	6	18	29	7	22	22	2	47
N	7	22	22	1	48	3	56	12	3	25	3	38	10	8	41	8	17	25	1	50
C	7	16	22	2	53	4	46	15	5	31	3	30	11	10	47	7	12	24	1	56
E	7	13	23	1	54	4	37	18	5	35	4	23	13	9	51	7	8	26	1	58
NE	7	12	28	1	52	4	28	28	5	35	5	21	17	9	49	7	8	29	1	55
AS	4	16	18	22	39	3	36	12	20	29	1	36	5	39	20	5	13	18	21	44
BoB	5	5	30	19	41	4	17	22	23	34	2	16	11	41	29	5	3	21	26	44

Table 5 Proportion of variations in AOD by the PBLH as inferred by the PRE

Location	Winter		Pre-monsoon		Monsoon		Post-monsoon	
	R^2	PRE	R^2	PRE	R^2	PRE	R^2	PRE
South	0.79	0.60	0.35	0.11	0.57	0.02	0.52	0
West	0.39	0.07	0.69	0.29	0.62	0.08	0.28	0.18
North	0.78	0.54	0.66	0.45	0.67	0.47	0.75	0.23
Central	0.57	0.01	0.40	0.33	0.48	0.14	0.76	0.06
East	0.66	0.54	0.57	0.46	0.53	0.25	0.55	0.04
North East	0.23	0.20	0.77	0.42	0.13	0.03	0.76	0.24
Arabian Sea	0.78	0.47	0.92	0.83	0.94	0.18	0.66	0.27
Bay of Bengal	0.81	0.46	0.92	0.92	0.83	0.56	0.96	0.43

the influence of meteorology in redistributing atmospheric particles over the region. The main conclusions are summarised as follows.

The distribution of aerosols shows large spatial variability with heavier loading over the IGP. Dust aerosols from the arid regions of Thar Desert are blown over northern India and are eventually spread over the Bay of Bengal. Similar to the foothills of the Himalayas and Tibetan Plateau, mountain ranges such as the Aravali, Eastern Ghats and the Western Ghats also exhibit spatial gradients with topographical differences. A region in central India bordered by mountain ranges on all four sides shows heavier aerosol loading suggesting the possibility of vertically advected aerosol layers due to surface hindrance but requires further analysis.

Meteorological parameters such as wind speed and divergence show seasonality with increased wind speed and convergence during the monsoon season. Monthly wind speeds and divergence correlate with AOD values both over the land and ocean suggesting an increased aerosol loading at higher wind speed which is converging to the region. However, there is an increased correlation in wind speeds at higher altitude with a maximum correlation at 850 hPa. The higher correlation was further investigated with backward trajectories at near surface (1000 hPa) and mid-tropospheric (850 hPa) levels describing the importance of wind direction and areal influence of wind trajectories. Apart from the seasonality in AOD, there is also evidence of increasing spatial variability suggesting the accumulation of increased aerosols to particular locations within the region. The Indian subcontinent being a host of varied climatology was further divided into subregions for the analysis. Correlation analysis between AOD and the meteorological parameters was carried out over each subregion. The results depict the influence of prevailing meteorological conditions on distributing various aerosol types over the subregions. In general, over the land, higher PBLH and higher wind speed support DU and SS aerosols, whereas lower PBLH and low wind speed support SU, BC and OC aerosols.

This may be because increased wind speed and higher PBLH result in increased surface wind stress and an unstable atmosphere with increased turbulence in turn supporting DU and SS aerosol production. Over the ocean, the transported continental aerosols are concentrated over regions of stable atmosphere as denoted by lower PBLH. Increasing wind speeds over the ocean results in an increased SS aerosol concentration over the region. Further, the influence of atmospheric diffusion is quantified by evaluating the PRE of a multiple linear regression model. The inclusion of PBLH in addition to wind speed and divergence shows significant PRE in most of the cases. This is particularly evident during the winter and pre-monsoon seasons where the PBLH explains almost 30 to 90% of the total variance in AOD over the subregions.

Publisher's note Springer Nature remains neutral with regard to jurisdictional claims in published maps and institutional affiliations.

References

Ainsworth EA, Long SP (2004) What have we learned from 15 years of free-air CO2 enrichment (FACE)? A meta-analytic review of the responses of photosynthesis, canopy properties and plant production to rising CO2. New Phytol 165:351–372. https://doi.org/10.1111/j.1469-8137.2004.01224.x

Aloysius M, Mohan M, Parameswaran K, George SK, Nair PR (2008) Aerosol transport over the Gangetic basin during ISRO-GBP land campaign-II. Ann Geophys 26:431–440. https://doi.org/10.5194/angeo-26-431-2008

Badarinath KVS, Kharol SK, Kaskaoutis DG, Sharma AR, Ramaswamy V, Kambezidis HD (2010) Long-range transport of dust aerosols over the Arabian Sea and Indian region - a case study using satellite data and ground-based measurements. Glob Planet Chang 72:164–181. https://doi.org/10.1016/j.gloplacha.2010.02.003

Cheng S, Chen D, Li J, Wang H, Guo X (2007) The assessment of emission-source contributions to air quality by using a coupled MM5-ARPS-CMAQ modeling system: a case study in the Beijing metropolitan region, China. Environ Model Softw 22:1601–1616. https://doi.org/10.1016/j.envsoft.2006.11.003

Chitranshi S, Sharma SP, Dey S (2015) Satellite-based estimates of outdoor particulate pollution (PM10) for Agra City in northern India. Air Qual Atmos Health 8:55–65. https://doi.org/10.1007/s11869-014-0271-x

Choudhry P, Misra A, Tripathi SN (2012) Study of MODIS derived AOD at three different locations in the Indo Gangetic Plain: Kanpur, Gandhi College and Nainital. Ann Geophys 30:1479–1493. https://doi.org/10.5194/angeo-30-1479-2012

Chylek P, Coakley JA (1974) Aerosols and climate. Science 183:75–77. https://doi.org/10.1126/science.183.4120.75

Dey S (2004) Influence of dust storms on the aerosol optical properties over the Indo-Gangetic basin. J Geophys Res 109:D20211. https://doi.org/10.1029/2004JD004924

Ding A, Wang T, Zhao M, Wang T, Li Z (2004) Simulation of sea-land breezes and a discussion of their implications on the transport of air pollution during a multi-day ozone episode in the Pearl River Delta of China. Atmos Environ 38:6737–6750. https://doi.org/10.1016/j.atmosenv.2004.09.017

Fuzzi S, Baltensperger U, Carslaw K, Decesari S, Denier van der Gon H, Facchini MC, Fowler D, Koren I, Langford B, Lohmann U, Nemitz E, Pandis S, Riipinen I, Rudich Y, Schaap M, Slowik JG, Spracklen DV, Vignati E, Wild M, Williams M, Gilardoni S (2015) Particulate matter, air quality and climate: lessons learned and future needs. Atmos Chem Phys 15:8217–8299. https://doi.org/10.5194/acp-15-8217-2015

Gautam R, Hsu NC, Lau K-M, Kafatos M (2009a) Aerosol and rainfall variability over the Indian monsoon region: distributions, trends and coupling. Ann Geophys 27:3691–3703. https://doi.org/10.5194/angeo-27-3691-2009

Gautam R, Hsu NC, Lau K-M et al (2009b) Enhanced pre-monsoon warming over the Himalayan-Gangetic region from 1979 to 2007. Geophys Res Lett 36:n/a-n/a. https://doi.org/10.1029/2009GL037641

Gelaro R, McCarty W, Suárez MJ, Todling R, Molod A, Takacs L, Randles CA, Darmenov A, Bosilovich MG, Reichle R, Wargan K, Coy L, Cullather R, Draper C, Akella S, Buchard V, Conaty A, da Silva AM, Gu W, Kim GK, Koster R, Lucchesi R, Merkova D, Nielsen JE, Partyka G, Pawson S, Putman W, Rienecker M, Schubert SD, Sienkiewicz M, Zhao B (2017) The modern-era retrospective analysis for research and applications, version 2 (MERRA-2). J Clim 30:5419–5454. https://doi.org/10.1175/JCLI-D-16-0758.1

Giles DM, Holben BN, Tripathi SN, Eck TF, Newcomb WW, Slutsker I, Dickerson RR, Thompson AM, Mattoo S, Wang SH, Singh RP, Sinyuk A, Schafer JS (2011) Aerosol properties over the Indo-Gangetic Plain: a mesoscale perspective from the TIGERZ experiment. J Geophys Res Atmos 116:1–19. https://doi.org/10.1029/2011JD015809

Global Modeling and Assimilation Office (GMAO) (2015a), MERRA-2 tavg1_2d_flx_Nx: 2d,1-Hourly,Time-Averaged,Single-Level, Assimilation,Surface Flux Diagnostics V5.12.4, Greenbelt, MD, USA, Goddard Earth Sciences Data and Information Services Center (GES DISC), Accessed: 20-10-2018. https://doi.org/10.5067/7MCPBJ41Y0K6

Global Modeling and Assimilation Office (GMAO) (2015b), MERRA-2 tavgM_2d_aer_Nx: 2d,Monthly mean, Time-averaged, Single-Level,Assimilation,Aerosol Diagnostics V5.12.4, Greenbelt, MD, USA, Goddard Earth Sciences Data and Information Services Center (GES DISC), Accessed: 20-10-2018. https://doi.org/10.5067/FH9A0MLJPC7N

Guleria RP, Kuniyal JC (2013) Aerosol climatology in the northwestern Indian Himalaya: a study based on the radiative properties of aerosol. Air Qual Atmos Health 6:717–724. https://doi.org/10.1007/s11869-013-0206-y

Guleria RP, Kuniyal JC (2016) Characteristics of atmospheric aerosol particles and their role in aerosol radiative forcing over the northwestern Indian Himalaya in particular and over India in general. Air Qual Atmos Health 9:795–808. https://doi.org/10.1007/s11869-015-0381-0

Guttikunda SK, Carmichael GR, Calori G, Eck C, Woo JH (2003) The contribution of megacities to regional sulfur pollution in Asia. Atmos Environ 37:11–22. https://doi.org/10.1016/S1352-2310(02)00821-X

Hoek G, Brunekreef B, Goldbohm S, Fischer P, van den Brandt PA (2002) Association between mortality and indicators of traffic-related air pollution in the Netherlands: a cohort study. Lancet 360: 1203–1209

Hsu NC, Jeong M-J, Bettenhausen C, Sayer AM, Hansell R, Seftor CS, Huang J, Tsay SC (2013) Enhanced deep blue aerosol retrieval algorithm: the second generation. J Geophys Res Atmos 118: 9296–9315. https://doi.org/10.1002/jgrd.50712

Judd CM, McClelland GH, Ryan CS (2009) Data analysis - a model comparison approach. Routledge, Abingdon

Kalapureddy MCR, Kaskaoutis DG, Ernest Raj P et al (2009) Identification of aerosol type over the Arabian Sea in the premonsoon season during the Integrated Campaign for Aerosols, Gases and Radiation Budget (ICARB). J Geophys Res Atmos 114: D17203. https://doi.org/10.1029/2009JD011826

Kaskaoutis DG, Kalapureddy MCR, Devara PCS, Kosmopoulos PG, Nastos PT, Krishna Moorthy K, Kambezidis HD (2009) Spatio-temporal aerosol optical characteristics over the Arabian Sea during the pre monsoon season. Atmos Chem Phys Discuss 9:22223–22269

Kaskaoutis DG, Kalapureddy MCR, Krishna Moorthy K, Devara PCS, Nastos PT, Kosmopoulos PG, Kambezidis HD (2010) Heterogeneity in pre-monsoon aerosol types over the Arabian Sea deduced from ship-borne measurements of spectral AODs. Atmos Chem Phys 10:4893–4908. https://doi.org/10.5194/acp-10-4893-2010

Kaskaoutis DG, Rashki A, Houssos EE, Legrand M, Francois P, Bartzokas A, Kambezidis HD, Dumka UC, Goto D, Takemura T (2017) Assessment of changes in atmospheric dynamics and dust activity over southwest Asia using the Caspian Sea-Hindu Kush Index. Int J Climatol 37:1013–1034. https://doi.org/10.1002/joc.5053

Kedia S, Ramachandran S, Holben BN, Tripathi SN (2014) Quantification of aerosol type, and sources of aerosols over the Indo-Gangetic Plain. Atmos Environ 98:607–619. https://doi.org/10.1016/j.atmosenv.2014.09.022

Lau KM, Ramanathan V, Wu GX, Li Z, Tsay SC, Hsu C, Sikka R, Holben B, Lu D, Tartari G, Chin M, Koudelova P, Chen H, Ma Y, Huang J, Taniguchi K, Zhang R (2008) The joint aerosol-monsoon experiment: a new challenge for monsoon climate research. Bull Am Meteorol Soc 89:369–383. https://doi.org/10.1175/BAMS-89-3-369

Levy RC, Remer LA, Kleidman RG, Mattoo S, Ichoku C, Kahn R, Eck TF (2010) Global evaluation of the Collection 5 MODIS dark-target aerosol products over land. Atmos Chem Phys 10:10399–10420. https://doi.org/10.5194/acp-10-10399-2010

Li Z, Rosenfeld D, Fan J (2017) Aerosols and their impact on radiation, clouds, precipitation, and severe weather events. Oxford University Press, Oxford

McNoldy BD (2004) Surface winds, divergence, and vorticity in stratocumulus regions using QuikSCAT and reanalysis winds. Geophys Res Lett 31:L08105. https://doi.org/10.1029/2004GL019768

Ministry of Shipping (2016) Annual report 2016-17, Ministry of Shipping India

Misra A, Jayaraman A, Ganguly D (2015) Validation of version 5.1 MODIS aerosol optical depth (deep blue algorithm and dark target approach) over a semi-arid location in Western India. Aerosol Air Qual Res 15:252–262. https://doi.org/10.4209/aaqr.2014.01.0004

Monkkonen P (2004) Relationship and variations of aerosol number and PM10 mass concentrations in a highly polluted urban environment - New Delhi, India. Atmos Environ 38:425–433. https://doi.org/10.1016/j.atmosenv.2003.09.071

Moorthy KK, Satheesh SK (2000) Characteristics of aerosols over a remote island, Minicoy in the Arabian Sea: optical properties and retrieved size characteristics. Q J R Meteorol Soc 126:81–109. https://doi.org/10.1002/qj.49712656205

Nair VS, Suresh Babu S, Krishna Moorthy K (2008) Spatial distribution and spectral characteristics of aerosol single scattering albedo over the Bay of Bengal inferred from shipborne measurements. Geophys Res Lett 35:1–5. https://doi.org/10.1029/2008GL033687

Pease PP, Tchakerian VP, Tindale NW (1998) Aerosols over the Arabian Sea: geochemistry and source areas for aeolian desert dust. J Arid Environ 39:477–496. https://doi.org/10.1006/jare.1997.0368

Penner JE et al (2001) Aerosols, their direct and indirect effects. In: Houghton JT et al (eds) Climate change 2001: the scientific basis, contribution of working group I to the third assessment report of the intergovernmental panel on climate change. Cambridge University Press, Cambridge, pp 289–348

Platnick, S., et al., 2017. MODIS atmosphere L3 monthly product. NASA MODIS Adaptive Processing System, Goddard Space Flight Center, USA. https://doi.org/10.5067/MODIS/MOD08_M3.061

Pope CA, Burnett RT, Thurston GD et al (2004) Cardiovascular mortality and long-term exposure to particulate air pollution. Circulation 109: 71–77. https://doi.org/10.1161/01.CIR.0000108927.80044.7F

Prospero JM (2002) Environmental characterization of global sources of atmospheric soil dust identified with the NIMBUS 7 Total Ozone Mapping Spectrometer (TOMS) absorbing aerosol product. Rev Geophys 40:1002. https://doi.org/10.1029/2000RG000095

Quan J, Gao Y, Zhang Q, Tie X, Cao J, Han S, Meng J, Chen P, Zhao D (2013) Evolution of planetary boundary layer under different weather conditions, and its impact on aerosol concentrations. Particuology 11:34–40. https://doi.org/10.1016/j.partic.2012.04.005

Rajeev K, Ramanathan V, Meywerk J (2000) Regional aerosol distribution and its long-range transport over the Indian Ocean. J Geophys Res Atmos 105:2029–2043. https://doi.org/10.1029/1999JD900414

Ramachandran S, Cherian R (2008) Regional and seasonal variations in aerosol optical characteristics and their frequency distributions over India during 2001–2005. J Geophys Res 113:D08207. https://doi.org/10.1029/2007

Ramanathan V, Crutzen PJ, Andreae MO (1990) Biomass burning in the tropics: impact on atmospheric chemistry and biogeochemical cycles. Science 250:1669–1678. https://doi.org/10.1126/science.250.4988.1669

Ramanathan V, Chung C, Kim D, Bettge T, Buja L, Kiehl JT, Washington WM, Fu Q, Sikka DR, Wild M (2005) Atmospheric brown clouds: impacts on South Asian climate and hydrological cycle. Proc Natl Acad Sci 102:5326–5333. https://doi.org/10.1073/pnas.0500656102

Rolph G, Stein A, Stunder B (2017) Real-time environmental applications and display system: READY. Environ Model Softw 95:210–228. https://doi.org/10.1016/j.envsoft.2017.06.025

Sayer AM, Hsu NC, Bettenhausen C, Jeong M-J (2013) Validation and uncertainty estimates for MODIS Collection 6 "Deep Blue" aerosol data. J Geophys Res Atmos 118:7864–7872. https://doi.org/10.1002/jgrd.50600

Schwartz SE (1996) The Whitehouse effect - shortwave radiative forcing of climate by anthropogenic aerosols: an overview. J Aerosol Sci 27: 359–382. https://doi.org/10.1016/0021-8502(95)00533-1

Seinfeld JHJH, Pandis SNSN (2006) Atmospheric chemistry and physics: from air pollution to climate change

Singh RP, Dey S, Tripathi SN, Tare V, Holben B (2004) Variability of aerosol parameters over Kanpur, northern India. J Geophys Res Atmos 109:1–14. https://doi.org/10.1029/2004JD004966

Srivastava N, Satheesh SK, Blond N, Moorthy KK (2016) Anthropogenic aerosol fraction over the Indian region: model simulations versus multi-satellite data analysis. Int J Remote Sens 37:782–804. https://doi.org/10.1080/01431161.2015.1136445

Stein AF, Draxler RR, Rolph GD, Stunder BJB, Cohen MD, Ngan F (2015) NOAA's HYSPLIT atmospheric transport and dispersion modeling system. Bull Am Meteorol Soc 96:2059–2077. https://doi.org/10.1175/BAMS-D-14-00110.1

Tanner PA, Law P (2002) Effect of synoptic weather systems upon the air quality in an Asian megacity. Water Air Soil Pollut 136:105–124. https://doi.org/10.1023/A:1015275404592

Tripathi SN, Dey S, Chandel A, Srivastava S, Singh RP, Holben BN (2005) Comparison of MODIS and AERONET derived aerosol optical depth over the Ganga Basin, India. Ann Geophys 23:1093–1101. https://doi.org/10.5194/angeo-23-1093-2005

Twomey S (1977) The influence of pollution on the shortwave albedo of clouds. J Atmos Sci 34:1149–1152

Wang C (2004) A modeling study on the climate impacts of black carbon aerosols. J Geophys Res Atmos 109:D3. https://doi.org/10.1029/2003JD004084

Wang X, Wang K, Su L (2016) Contribution of atmospheric diffusion conditions to the recent improvement in air quality in China. Sci Rep 6:36404. https://doi.org/10.1038/srep36404

Washington R, Todd M, Middleton NJ, Goudie AS (2003) Dust-storm source areas determined by the total ozone monitoring spectrometer and surface observations. Ann Assoc Am Geogr 93:297–313. https://doi.org/10.1111/1467-8306.9302003

WHO (2013) Research for universal health coverage: world health report 2013

Zhao C, Wang Y, Yang Q et al (2010) Impact of East Asian summer monsoon on the air quality over China: view from space. J Geophys Res 115:D09301. https://doi.org/10.1029/2009JD012745

Zheng XY, Fu YF, Yang YJ, Liu GS (2015) Impact of atmospheric circulations on aerosol distributions in autumn over eastern China: observational evidence. Atmos Chem Phys 15:12115–12138. https://doi.org/10.5194/acp-15-12115-2015

Ziomas IC, Melas D, Zerefos CS, Bais AF, Paliatsos AG (1995) Forecasting peak pollutant levels from meteorological variables. Atmos Environ 29:3703–3711. https://doi.org/10.1016/1352-2310(95)00131-H